



Communication

Reversible adhesion surface coating proppant

Quan Xu^a, Fan Fan^a, Zhaohui Lu^{b,*}, Mao Sheng^a, Shouceng Tian^a, Ye Zhang^b,
Linhua Pan^b, Yang Zhou^{a,*}

^a State Key Laboratory of Petroleum Resources and Prospecting, Beijing Key Laboratory of Biogas Upgrading Utilization, Harvard SEAS-CUPB Joint Laboratory on Petroleum Science, China University of Petroleum (Beijing), Beijing 102249, China

^b National Joint Engineering Research Center for Shale Gas Exploration and Development, Chongqing Institute of Geology and Mineral Resources, Chongqing 401120, China



ARTICLE INFO

Article history:

Received 20 January 2020

Received in revised form 5 February 2020

Accepted 10 February 2020

Available online 10 February 2020

Keywords:

Self-suspension

Coating

Proppants

Hydraulic fracturing process

Liquid conductivity

ABSTRACT

Proppant is a key material in the hydraulic fracturing process, which has been widely used in unconventional oil exploitation. Normal proppants are easy to sedimentate and accumulate at the entrance of shale fracture, which will block the diversion of water, oil and gas. Coated proppants (CPs) are fabricated by coating resin on normal ceramic proppants through a simple method, which is dramatically enhanced the supporting properties in shale fracture and easy to scale up. Compared with uncoated ceramic proppants, the self-suspension ability of CPs is ~ 11 times higher, which are able to migrate and distribute farther and deeper inside the fracture. At the same time, Coating enhanced the 23.7% of adhesive force in maximum, which makes the CPs easier to adhere on the fracture surface to support the shale fracture. Besides, the liquid conductivity of CPs is 60% higher than uncoated ceramic proppants at 13.6 MPa pressure. This method is expected to fabricate varieties of proppants for shale fracture supporting to improve the exploration of unconventional oil and gas resources.

© 2020 Chinese Chemical Society and Institute of Materia Medica, Chinese Academy of Medical Sciences. Published by Elsevier B.V. All rights reserved.

The United States has launched a global revolution in shale gas development, with explosive growth in gas production [1,2]. The shale gas resources potential of China is comparable to that of the United States [3–5]. Exploration and development of shale gas can greatly ease the pressure on Chinese natural gas demand, and improve Chinese energy structure and energy security at the same time [6–8]. At present, China Petroleum and Chemical Corporation has achieved a breakthrough in shale gas exploration and development in the Fuling area of Chongqing [9]. At the end of 2016, a national-level shale gas demonstration zone with a production ability of $100 \times 10^8 \text{ m}^3$ and a cumulative production of about $75 \times 10^8 \text{ m}^3$ has been demonstrated, indicating that Chinese Shale gas has excellent prospects for exploration and development [10–13]. Hydraulic fracturing (HF) is considered to be the main and effective method to improve oil and gas recovery [3,14]. In the process of hydraulic fracturing, in order to prevent the fracture from re-closing under formation closing pressure, proppants are required to support the fracture [15,16]. Proppant are carried by the fracturing fluid and stacked in the fractures,

thereby forming artificial fractures with a certain liquid conductivity [17]. A variety of proppants have been used in hydraulic fracturing, such as metal aluminum balls, walnut shells, glass beads, plastic balls, etc. Due to strength, hardness and cost reasons, these proppants are basically no longer used [18]. At present, the proppants used in shale fracture supporting are mainly quartz sand, ceramic and resin-coated proppants [19].

Quartz sand is a solid, wear-resistant, chemically stable silicate mineral. The price is relatively low and it has a good production increase effect in low-closed pressure reservoirs [20]. Quartz sand is widely used in shallow wells within 1500 m, but it starts to break at about 20 MPa because compressive strength is low [21–23]. At the same time, its sphericity is low, which will cause larger wear on fracturing strings, pump heads and perforations [24]. Therefore, more ceramic proppants are used for deep wells. Ceramic proppants generally use bauxite as raw material and is obtained by sintering with additives such as pyrite and dolomite [25]. Its density is closely related to the content of Al_2O_3 . As the content of Al_2O_3 increases, the density becomes larger. Although ceramic proppants have larger strength, they have the disadvantages of high density, large cost and big construction risk [18]. The resin-coated proppants combine the advantages of quartz sand and ceramic proppants, with higher sphericity and lower density, which are able to prevent the proppants reflow. The surfaces of the

* Corresponding authors.

E-mail addresses: luzhaohui929@126.com (Z. Lu), zhouyang@cup.edu.cn (Y. Zhou).

proppants are uneven, which have a large number of open pores and pits [26]. When the proppants are coated, the resin fills or covers the pits and open pores. At the same time, due to the lower density of the resin, the density of the reducing proppants backflow, and preventing proppants from being embedded in the stratum [27,28]. The salient features of resin-coated proppants are low density, strong resistance to crushing, and embedding prevention [29].

In this work, we have fabricated self-suspension proppants successfully in a simple way, which is easy to scale up for mass production. The self-suspension proppants have a core-shell structure, a porous resin layer acts a shell coated on the ceramic core (Fig. 1a), which has excellent liquid conductivity compared with normal ceramic proppants without coating. At the same time, the self-suspension ability of the CPs is ~ 11 times higher than normal ceramic proppants. Due to the high density, uncoated normal ceramic proppants supposed to sediment at the entrance of shale fracture (Fig. 1b). The CPs supposed to go deeper inside the shale fracture, due to its self-suspension ability (Fig. 1c). A support plate test was conducted between the new self-suspension proppants and commercial coated proppants, that the new self-suspension proppants have better migration and distribution in shale fracture. Compared with commercial proppants was reduced. The development trend of fracturing proppants is toward low density, high strength, coated ceramic proppants, the self-suspension proppants are able to go deeper in the shale fracture, easier to adhere to the fracture surface to improve the fracture supporting ability.

Figs. S1a and b (Supporting information) are scanning electron microscope (SEM) photographs of the surface morphology of ceramic proppant, which is rough and the porous structure can be observed. SEM photographs of the CP are shown in Figs. S1c and d (Supporting information). The resin shell coated on the ceramic proppant decreased the roughness of pure ceramic proppant surface significantly. The surface of the CP is smoother, with sphericity close to 1.

As shown in the energy-dispersive X-ray spectroscopy (EDX) results of uncoated proppant (Fig. 2a), aluminum (Fig. 2b) and silicon (Fig. 2c) elements can be observed on the surface, while no carbon (Fig. 2d) element. For the CP, silicon (Figs. 2e and f) and aluminum (Fig. 2g) elements were almost undetectable, while carbon can be observed on the surface (Fig. 2h). The EDX mapping confirm that resin has been coated on the surface of uncoated proppant, since no aluminum and silicon are detected on the surface of CP.

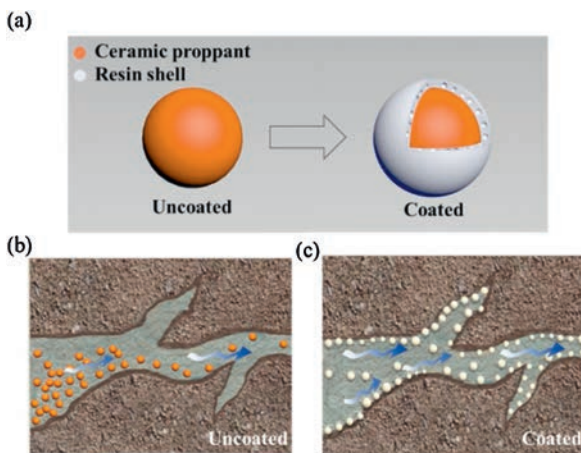


Fig. 1. Self-suspension properties and structure of coated proppant. (a) Film structure of proppant; (b) Schematic diagram of uncoated proppants in shale fractures; (c) Schematic diagram of CPs (coated) in shale fractures.

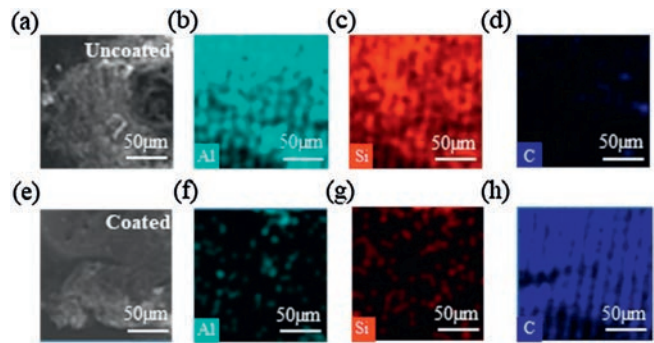


Fig. 2. EDX mapping of the uncoated proppant and CP. (a, e) SEM image of the uncoated proppant and CP. (b, f) Aluminum on the surface of the uncoated proppant and CP. (c, g) Silicon on the surface of the uncoated proppant and CP. (d, h) Carbon on the surface of the uncoated proppant and CP.

Fig. 3a displays the liquid conductivity of the proppants under different effective closure stress changed from 6.9 MPa to 27.6 MPa, while the proppants concentration and flow were fixed at 6 kg/m^2 and 3 mL/min . Although the conductivity of both the coated proppants and the uncoated proppants decreased with increasing closure stress, the liquid conductivity of the coated proppants was higher than the uncoated proppants at lower closure pressure. The liquid conductivity of the self-suspension proppants was 60% higher than uncoated ceramic proppants at 13.8 MPa. When the closure stress reached about 26 MPa, the liquid conductivity of the coated proppants was similar to that of the uncoated proppants. This indicates that the proppant coating is able to improve its liquid conductivity effectively. As discussed above, the surface

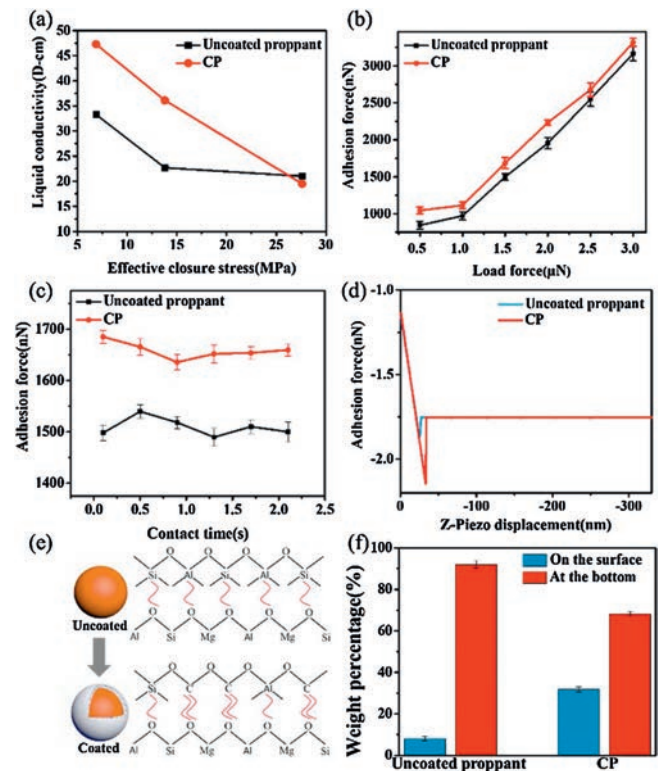


Fig. 3. (a) Liquid conductivity of the CPs and uncoated proppants under different closure pressure. (b) Adhesion performance of the CPs and the uncoated proppants surface of different load force. (c) Adhesion performance of the CPs and the uncoated proppants surface of different contact time. (d) Typical AFM force curve in adhesion measurement for a load force of $2 \mu\text{N}$ and a contact time of 0.1 s. (e) Mechanism diagram of adhesion force of the CPs and uncoated proppants. (f) Results of the CPs and uncoated proppants sedimentation experiment.

coating reduced the roughness of ceramic proppants, which able to increase the liquid flow ability. Besides, the resin is a hydrophobic polymer, which can provide a coating with excellent shear strength and make the liquid flow better, therefore improve the liquid conductivity ability [30].

The adhesive ability of self-suspension proppants was conducted by atomic force microscopy (AFM). Fig. 3b gives the variations of adhesion forces under different load force conditions, and the contact time was fixed at 0.1 s. With the load force increased from 0.5 μN to 3 μN , the adhesion force of CPs is larger than uncoated proppants in each testing load force, which is 23.69%, 14.59%, 12.47%, 14.06%, 4.87%, 4.76% higher, respectively. With the increase of the load force, the adhesion of the coated and uncoated proppants increased, and the trend remained the same, which showed that the coating did not change the relationship between the proppant's adhesion force and the load force. But under the same conditions, the adhesion force of the CPs is higher than that of the uncoated proppants. The contact time *versus* adhesion force is shown in Fig. 3c, where the contact time increased from 0.1 s to 2.1 s, while the load force was kept as 1.5 μN . When the contact time was changed, there was no significant change in the adhesion force between the coated and uncoated proppants, but the adhesion of CPs is improved compared with uncoated proppants. The adhesion forces of coated proppants changed by 12.47%, 8.17%, 7.74%, 10.90%, 9.50%, 10.63%, compared with the uncoated proppants, respectively. After the test, the proppants were not significantly deformed. The effect of the local deformation of the particles can be safely ignored. Since the load force and contact time did not cause chemical changes inside of the proppants sample, the surface adhesion force is affected by the film of coated proppants. The resin coating of the proppants coat increases the adhesion, and the proppants will more easily adhere to the surface of the fracture. At the same time, the resin coating will also cause the proppants to form inter-particle adhesion, thereby improving the fracture supporting ability. The typical AFM force (known as force curve) is illustrated in Fig. 3d, the adhesion force is determined by the difference of extended and retract force curves. CPs have higher adhesion force than uncoated proppants, this may be beneficial for improving the liquid conductivity of proppants.

EDX analysis proved that the coated proppants contained a large quantity of carbon (Fig. 2). Both silicon and aluminum in uncoated proppants form covalent bonds with oxygen, and the force between the proppants and the fracture surface is mainly van der Waals force. Since van der Waals forces are weak, short-range electrostatic attractive forces between uncharged molecules. The adhesion forces between uncoated proppants and fracture surface are weak. Once proppants were coated, carbon element would have a free pair of electron pairs, which could form chemical bonds with oxygen on the fracture surface, including cohesive bonds and hydrogen bonds. Besides, as the temperature of underground rock fractures rises, force of chemical bond between carbon and oxygen further increases [31–33]. As the strength of the chemical bond is much higher than the van der Waals force, the adhesion of the coated proppants has been increased and thus become higher than the uncoated proppants (Fig. 3e) [34–36].

To test the self-suspension ability of the CPs, the sedimentation experiment was designed (Fig. 3f). In the sedimentation experiment, the proppants were poured into guar gum solution (0.2 wt%) without any stirring. After standing for 5 min, 8.09 wt% of the uncoated proppants suspended on the surface of the guar gum solution, and the weight of the uncoated proppants on the bottom of the solution was 91.91 wt%. (Figs. S2a and b in Supporting information). The weight of the coated proppants suspended on the surface and the bottom of the guar gum solution was 31.82 wt% and 68.18 wt%, respectively (Figs. S2c and d in Supporting

information). The self-suspending ability (proppant weight on the surface/proppant weight at the bottom) of the coated proppants and uncoated proppants is 0.466 and 0.088, respectively. The self-suspension ability of the coated proppants has reached nearly 11 times that of the uncoated proppants.

After demonstrating the improvement of self-suspension performance, the CPs supposed has better migration and distribution between shale fracture. Another commercialized coated ceramic proppant, which have the similar size as CPs was selected to perform the migration and distribution experiments. Normally, ceramic based proppants will sediment fast to generate sand hill at the entrance of fracture. Figs. 4a and d are the photographs of the proppants migration and distribution experiment results of CPs and commercial coated proppants deposition in the plates at flow rates of 6 m^3/h and 9 m^3/h , respectively. As shown in the Figs. 4b and e, the uncoated proppants tend to sedimentate at the entrance of shale fracture while the CPs migration distance is farther. Figs. 4c and f show the bar graphs of the maximum height of proppants deposition in each plate in the primary fracture of the CPs and the commercial coated proppants under the different flow of 6 m^3/h and 9 m^3/h , respectively. According to Figs. 4c and f, in the primary fracture under the flow of 6 m^3/h , the CPs and commercial coated proppants had the maximum deposition height of 21.8 and 27.8 cm both in the fourth plate, and the minimum deposition height of 3.3 and 7.9 cm both in the ninth plate. When the injection flow increased, the average height of the proppants increased and the migration distance became longer. In the primary fracture under the flow of 9 m^3/h , the CPs had the maximum height of 17.7 cm in the fifth plate and the minimum height of 14 cm, appears in the ninth plate. However, the maximum height of the commercial coated proppants was 24.4 cm in the fourth plate. The minimum height that appeared in the ninth plate is 11.1 cm. The CPs successfully

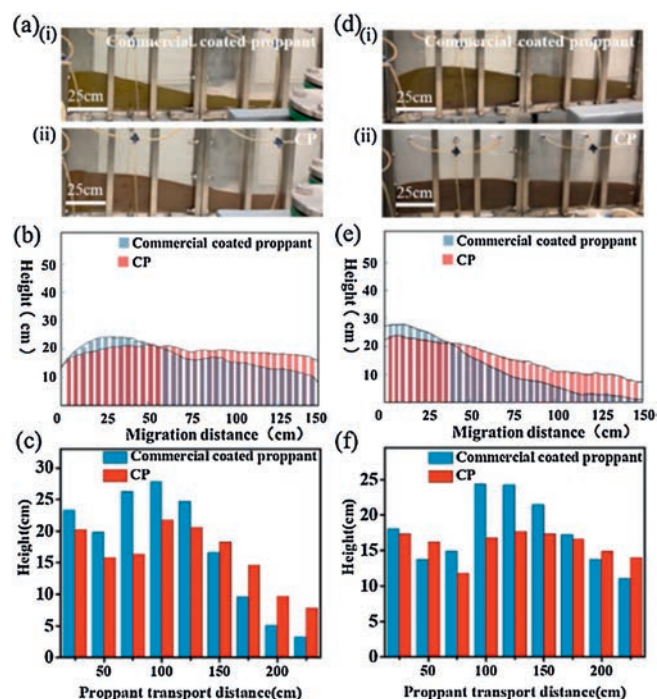


Fig. 4. Photograph of the commercial coated proppants (i) and the CPs (ii) spread result under the flow of (a) 6 m^3/h and (d) 9 m^3/h . Migration and distribution trend chart of the commercial coated proppants and the CPs under the flow of (b) 6 m^3/h and (e) 9 m^3/h . Bar graph of the CPs and the commercial coated proppants spread results under the flow of (c) 6 m^3/h and (f) 9 m^3/h .

reduced 21.6% and 27.5% maximum height of sand hill compared with commercial proppants.

Fig. S3 (Supporting information) shows the height change percentage of the proppants under various flow. In the primary fracture, the height changes of CPs and commercial coated proppants were 63.8% and 88.1% under the flow of $6\text{ m}^3/\text{h}$ according to the data. And the height change of the CPs was 20.9%, while the height change of the commercial coated proppants was 54.5% under the flow of $9\text{ m}^3/\text{h}$. The height changes of the discussion above indicated that CPs were able to go further and deeper in shale fracture, while more commercial proppants sedimented and accumulated at the entrance of fractures, which is due to the self-suspension ability of resin coating.

The stability and durability of CP were tested. Fig. S4 (Supporting information) shows the results of the self-suspension ability of CPs and uncoated ceramic proppants after different temperature ($40\text{--}80\text{ }^\circ\text{C}$) and pH ($1\text{--}13$) treatment. The changes of weight percentage of CPs and ceramic proppants on the surface of guar gum solution were negligible. The self-suspension ability of the CPs remains larger than the uncoated proppants. The sedimentation experiment confirms that the CPs are relatively stable within a certain temperature and pH range.

In conclusion, we have fabricated novel coated proppants, where the fabrication method is straight forward and easy to scale up. The self-suspension ability of the coated proppants is nearly 11 times that of the uncoated proppants. In addition, the adhesion force of the proppants is also enhanced, it is easier to adhere to the fracture surface, which is more promising for fracture supporting usage to increase the liquid conductivity of oil and gas flow. The proppants migration and distribution experiment proved that the CPs have better migration and distribution in the fracture. At the same time, CPs are able to go deeper into the fracture, which is due to its self-suspension ability. Our design is versatile and adaptable to a variety of proppants and expected to be applied to shale fractures.

Declaration of competing interest

The authors declare that they have no known competing financial interests or personal relationships that could have appeared to influence the work reported in this paper.

Acknowledgments

This research was supported by National Natural Science Foundation of China (Nos. 51875577, 51604050), Science Foundation

of China University of Petroleum, Beijing (Nos. 2462019QNXZ02, 2462019BJRC007), Chongqing Science and Technology Innovation Talent Support Program (No. CSTCCXLJRC201712).

Appendix A. Supplementary data

Supplementary material related to this article can be found, in the online version, at doi:<https://doi.org/10.1016/j.ccl.2020.02.014>.

References

- [1] J. Zhang, L. Ouyang, D. Zhu, A.D. Hill, *J. Petrol. Sci. Eng.* 130 (2015) 37–45.
- [2] R.J. Beckwith, *J. Petrol. Technol.* 63 (2011) 36–41.
- [3] Q. Li, H. Xing, J. Liu, X. Liu, *Petroleum* 1 (2015) 8–15.
- [4] Y. Yang, L. Wang, Y. Fang, C. Mou, *Renew. Sust. Energy Rev.* 76 (2017) 1465–1478.
- [5] Y. Li, Y. Li, B. Wang, Z. Chen, D. Nie, *Renew. Sust. Energy Rev.* 59 (2016) 420–428.
- [6] A. Reinicke, E. Rybacki, S. Stanchits, E. Huenges, G. Dresen, *Geochem.* 70 (2010) 107–117.
- [7] C. Zou, D. Dong, S. Wang, et al., *Petrol. Explor. Dev.* 37 (2010) 641–653.
- [8] Y. Zou, X. Ma, S. Zhang, et al., *Energy Technol. -Ger.* 3 (2015) 1233–1242.
- [9] X. Liu, W. Zeng, L. Liang, J. Xiong, *Petroleum* 2 (2016) 54–60.
- [10] M. Zoveidavianpoor, A. Gharibi, *J. Nat. Gas. Sci. Eng.* 24 (2015) 197–209.
- [11] C. Jia, M. Zheng, Y. Zhang, *Petrol. Explor. Dev.* 39 (2012) 139–146.
- [12] Y. Liu, X. Li, Q. Zhang, *Angew. Chem. Int. Ed.* 59 (2020) 1718–1726.
- [13] S.R. Kelemen, M. Afeworki, M.L. Gorbaty, et al., *Energy Fuel.* 21 (2007) 1548–1561.
- [14] A. Kondash, A. Vengosh, *Environ. Sci. Tech. Lrt.* 2 (2015) 276–280.
- [15] A.R. Rickards, H.D. Brannon, W.D.J.S.P. Wood, *Spe. Prod. Oper.* 21 (2006) 212–221.
- [16] S. Shiozawa, M. McClure, *J. Petrol. Sci. Eng.* 138 (2016) 298–314.
- [17] J. Bao, H. Liu, G. Zhang, et al., *Petrol. Explor. Dev.* 44 (2017) 306–314.
- [18] Q. Wen, S. Wang, X. Duan, et al., *J. Nat. Gas Sci. Eng.* 33 (2016) 70–80.
- [19] L. Fu, G. Zhang, J. Ge, et al., *Colloids Surf. A Physicochem. Eng. Asp.* 507 (2016) 18–25.
- [20] X. Ma, Y. Tian, Y. Zhou, et al., *Mater. Lett.* 180 (2016) 127–129.
- [21] F. Liang, M. Sayed, G.A. Al-Muntasheri, F.F. Chang, L. Li, *Petrol* 2 (2016) 26–39.
- [22] C. Zou, Y. Ni, J. Li, et al., *Sci. Total Environ.* 630 (2018) 349–356.
- [23] Y. Yu, Q. Xu, S. He, et al., *Coord. Chem. Rev.* 387 (2019) 154–179.
- [24] W. Zheng, S.C. Silva, D.D. Tannant, *J. Nat. Gas. Sci. Eng.* 53 (2018) 125–138.
- [25] R. Moghadasi, A. Rostami, A. Hemmati-Sarapardeh, *Adv. Geo-Energ. Res.* 3 (2019) 198–206.
- [26] Z.Y. Zhu, K.L. Xiang, Y.Z. Zhao, L. Li, X. Wang, *Mater. Sci. Forum.* 847 (2016) 527–531.
- [27] T. Chen, G.Z. Wang, J. Gao, et al., *Adv. Mater. Res.* 524–527 (2012) 1910–1914.
- [28] J. Fan, T.P. Bailey, Z. Sun, et al., *J. Petrol. Sci. Eng.* 163 (2018) 100–109.
- [29] W. Horadam, N. Venkat, T. Tran, et al., *J. Appl. Polym. Sci.* 131 (2014) 40735.
- [30] S. Irie, J. Rappolt, *Phenolic Resins: A Century of Progress*, Springer, 2010, pp. 503–515.
- [31] S. Tian, X. Dong, T. Wang, et al., *Langmuir* 34 (2018) 13882–13887.
- [32] Q. Xu, R. Zhang, M. Sheng, et al., *Chin. Chem. Lett.* 31 (2020) 1616–1619.
- [33] Q. Xu, M. Li, L. Zhang, J. Niu, Z. Xia, *Langmuir* 30 (2014) 11103–11109.
- [34] Q. Xu, Y. Wan, T.S. Hu, et al., *Nat. Commun.* 6 (2015) 8949.
- [35] M. Li, Q. Xu, X. Wu, et al., *ACS Appl. Mater. Interfaces* 10 (2018) 26787.
- [36] X. Dong, H. Zhao, Y. Mi, et al., *Chin. Chem. Lett.* 30 (2019) 2333–2337.